ELSEVIER

Thermochimica Acta 361 (2000) 1–20

thermochimica acta

www.elsevier.com/locate/tca

Temperature, heat and heat flow rate calibration of scanning calorimeters in the cooling mode☆

Stefan M. Sarge[a,*], Günther W.H. Höhne[b], Heiko K. Cammenga[c], Walter Eysel[d,1], Eberhard Gmelin[e]

[a]*Physikalisch-Technische Bundesanstalt, Bundesallee 100, D-38116 Braunschweig, Germany*
[b]*Universität Ulm, Albert-Einstein-Allee 11, D-89069 Ulm, Germany*
[c]*Technische Unversität Braunschweig, Hans-Sommer-Straße 10, D-38106 Braunschweig, Germany*
[d]*Universität Heidelberg, Im Neuenheimer Feld, D-69210 Heidelberg, Germany*
[e]*Max-Planck-Institut für Festkörperforschung, Heisenbergstraße 1, D-70569 Stuttgart, Germany*

Received 9 December 1999; accepted 16 December 1999

Abstract

The current publication continues the series of recommendations of the 'Calibration' Working Group of the German Society for Thermal Analysis (GEFTA) for temperature, heat and heat flow rate calibration of scanning calorimeters. It deals with calibration in the cooling mode. The procedures to be applied are essentially identical to those applied in the heating mode. Due to the general occurrence of supercooling for first-order phase transitions during cooling, liquid crystals and substances with higher-order phase transitions are recommended for temperature calibration. Substances with weak supercooling or substances for which the temperature dependence of the transformation enthalpy is known are recommended for heat calibration. The thermodynamic fundamentals relevant to the temperature dependence of phase transition enthalpies and phase transition temperatures are discussed. Detailed examples make it easy to follow the recommendations.

Keywords: Differential scanning calorimeter; DSC; Calibration; Temperature calibration; Heat calibration; Heat flow rate calibration; Calibration in the cooling mode; Supercooling; Liquid crystal

1. Purpose and scope of the recommendation

The present recommendation makes it possible to correctly carry out temperature, heat and heat flow rate calibrations of scanning calorimeters[2] in the cooling mode independently of the type of instrument; i.e. with the sample being subjected to a temperature program with defined cooling rate. Temperature calibration is feasible in the temperature range from 700

☆ Recommendation of the Working Group 'Calibration of scanning calorimeters' of the Gesellschaft für Thermische Analyse e.V. (GEFTA), Germany. Offprints can be obtained from the GEFTA office: Prof. Dr. V. Krämer, Kristallographisches Institut der Universität Freiburg, Hebelstraße 25, D-79104 Freiburg. A German version of this paper has been published in PTB-Mitteilungen 109 (1999) 357–375.

* Corresponding author. Fax: +49-531592-3205.
E-mail address: stefan.sarge@ptb.de (S.M. Sarge).

[1] Deceased.

[2] 'Scanning calorimetry' covers, among other things, differential scanning calorimetry (DSC).

0040-6031/00/$ – see front matter
PII: S0040-6031(00)00543-8

Nomenclature

a, b, c, d	coefficients for fitting polynomials
A	peak area
c_1	constant
cal	index: calibration sample
C_p	heat capacity at constant pressure
d	operator for total differentiation
eq	index: equilibrium
fus	index: fusion
G	free enthalpy (Gibbs' energy)
H	enthalpy
i	counting index
I	isotropic (liquid crystal phase)
K	calibration factor
K_Φ	calibration factor for heat flow rate measurements
K_Q	calibration factor for heat measurements
liq	index: liquid
lq	liquid (phase)
m	mass
N	nematic (liquid crystal phase)
p	pressure
q_{trs}	specific transition heat
Q	heat
Q_m	measured heat
Q_{tr}	true sample heat
R_{th}	thermal resistance
s	solid (phase)
s	index: solid
S	index: sample
S_A	smectic A (liquid crystal phase)
S	entropy
t	time
t_{end}	temperature program end time
t_f	final peak time
t_i	initial peak time
t_{st}	temperature program starting time
T	thermodynamic temperature
T_e	extrapolated peak-onset temperature
T_p	peak extremum temperature (peak maximum or peak minimum temperature)
tr	index: true
trs	index: transition
V	volume

Greek letters

α	expansion coefficient; angle
β	heating rate
∂	operator for partial differentiation
δ	operator for incomplete differentiation
Δ	operator for difference formation
ΔT	temperature difference
ϑ	Celsius temperature
κ	compressibility coefficient
Φ_{bl}	baseline heat flow rate
Φ_d	displayed heat flow rate
Φ'_0	displacement-corrected zero line heat flow rate
Φ'_d	displacement-corrected displayed heat flow rate
Φ_i	interpolated isothermal heat flow rate
$\Phi_{iso,end}$	isothermal end line
$\Phi_{iso,st}$	isothermal starting line
Φ_m	measured heat flow rate
τ	time constant
ξ	variable reaction term

to 200 K by means of the calibration materials recommended here; heat calibration is feasible between 850 and 100 K and heat flow rate calibration between 2250 and 20 K.

After reference to the relevant documents in Section 2, Section 3 gives the procedures for the calibration. Section 4 contains a list of suitable substances together with the necessary requirements and the rationale for the selection as well as some advice for their use. Section 5 (Annex) contains detailed examples and a survey of theoretical and thermodynamic fundamentals, particularly valid for the cooling mode. The symbols used are given in box.

As a principle, the results of a calibration in the cooling mode are different from those obtained in the heating mode, as the temperature distribution in the calorimeter is asymmetrical with respect to heating and cooling. This asymmetry is due to the fact that the heat transfer is not linearly dependent on the temperature difference, so that different heat flux densities are formed during heating and cooling, leading to different heat and heat flow rate calibration factors. These

effects typically are small so that in a first approximation a calorimeter symmetric with respect to heating and cooling can be assumed. The procedures recommended here mainly serve to verify and check this symmetry at regular intervals and to determine correction values, if need be.

When conventional calibration substances are used for temperature calibration in the cooling mode, supercooling of the relevant phase transition has to be coped with.

A prerequisite for the application of this recommendation is the correct and complete calibration of the device *in the heating mode* in accordance with the recommendations already published (see Section 2).

2. Documents to be taken into account

When these recommendations are applied, the following publications of the GEFTA Working Group for Calibration of Scanning Calorimeters in the heating mode are to be taken into account:

- G.W.H. Höhne, H.K. Cammenga, W. Eysel, E. Gmelin, W. Hemminger, The temperature calibration of scanning calorimeters, Thermochim. Acta 160 (1990) 1–12.
- H.K. Cammenga, W. Eysel, E. Gmelin, W. Hemminger, G.W.H. Höhne, S.M. Sarge, The temperature calibration of scanning calorimeters. Part 2. Calibration substances, Thermochim. Acta 219 (1993) 333–342.
- S.M. Sarge, E. Gmelin, G.W.H. Höhne, H.K. Cammenga, W. Hemminger, W. Eysel, The caloric calibration of scanning calorimeters, Thermochim. Acta 247 (1994) 129–168.

The documents referred to in these publications on the International Temperature Scale, standards and the nomenclature are also to be taken into account.

3. Procedure

The procedures to be applied comprise a check whether the calibration performed in the heating mode is also valid in the cooling mode and, in the event of an asymmetry being found, a separate calibration for this mode.

3.1. Temperature calibration

3.1.1. Rationale for the procedure

As the supercooling in the transition is different and in most cases not reproducible for the various usual temperature calibration substances (see Section 4), calibration substances with defined phase transition temperatures, which completely comply with the requirements for calibration substances are not available (see Section 4.1). This is why an independent temperature calibration in the cooling mode is not possible by the classical procedure. What is possible is just a check of the symmetry of the two temperature scales relative to the calibration previously performed in the heating mode. Special calibration substances are not needed for this relative calibration. Instead, pure substances whose transitions do not tend to supercooling, if possible, or have only a small and well-defined supercooling effect are sufficient.

As for phase transitions of non-first order, an evaluation different from that used for the heating mode is necessary. Here, the peak extremum whose position depends not only on the heating rate applied but also on the sample mass — according to a non-linear law — should be evaluated (see Section 5.2.2).

3.1.2. Check of the symmetry

- From the list of the calibration substances recommended (Table 1) a substance is selected, whose phase transition temperature lies within the range of interest.
- A sample of this substance is weighed in; its mass should roughly be equal to that recommended for the respective calorimeter and used for routine measurements.
- With this sample the transition is to be measured at three heating and three cooling rates. At least two experiments are to be performed for each heating and cooling rate. It is to be taken into account when selecting cooling rates, that these are really achieved by the respective instrument.
- For each of the peaks obtained, in accordance with Table 1 the extrapolated peak-onset temperature T_e or the peak extremum temperature T_p is determined. The extrapolated peak-onset temperature T_e is defined as the temperature of the intersection

Table 1
Substances recommended for temperature calibration in the cooling mode

Substance	Transition	Evaluation T_e or T_p	Phase transition temperature		Supercooling ΔT (K)	Literature
			ϑ_{trs} (°C)	T_{trs} (K)		
Adamantane	s↔s	T_e	−64.49[e]	208.66[e]	<1	[1,2,20]
M24[a]	S_A↔N	T_p	66	339	<0.5	[3]
HP-53[b]	S_A↔N	T_p	116	389		
BCH-52[c]	N↔I	T_p	162	435		
Indium	s↔lq	T_e	156.6	429.8	<2	[4]
$NaNO_3$	s↔s	T_p	276	549	<0.5	[5]
Zn[d]	s↔lq	T_e	419.5[f]	692.7[f]		[6]

[a] 4-Cyano-4′-octyloxybiphenyl.
[b] 4-(4-Pentyl-cyclohexyl)-benzoic acid-4-propyl-phenyl ester.
[c] 4′-Ethyl-4-(4-propyl-cyclohexyl)-biphenyl.
[d] Zn very easily reacts with aluminium which is usually used as crucible material (also when carefully oxidised). To avoid alloy formation with potential subsequent destruction of calorimeter components, it is therefore necessary to proceed very carefully and with great attention. It is advised to use only fresh samples, to examine the crucible bottom for cracks in the aluminium oxide layer, and to immediately cut short a series of experiments as soon as during successive experiments an increase in the peak width or a decrease of the peak area is observed. The authors do not accept any responsibility for damages!
[e] ITS-48 value converted to ITS-90.
[f] IPTS-68 value converted to ITS-90.

of the auxiliary line through the leading edge of the peak with the linearly extrapolated initial baseline, the peak extremum temperature T_p as the temperature of the extremum (maximum in heating, minimum in cooling) of the difference between curve of measured values and interpolated baseline.

- It is to be checked whether the temperatures thus obtained in the first and second experiments differ significantly.
- If this is not the case, T_e is plotted as a function of the heating rate, and T_p as a function of the square root of the product of heating rate and sample mass (cooling rates count negative). Regression lines are determined separately for the heating and cooling sections and these are each extrapolated to the heating rate zero. The temperature values obtained in that way are compared with the respective true temperatures T_{tr}, taking the supercooling to be expected into account.
- If the difference obtained differs significantly from the supercooling stated in Table 1, this indicates an instrumental asymmetry leading to different corrections for the heating and the cooling mode. In that case, a separate calibration is to be performed for the cooling mode (see Section 3.1.3).

3.1.3. Performance of the calibration

- From the list of the calibration substances recommended (Table 1), three substances are selected, which should have as different phase transition temperatures as possible in the temperature range in question.
- Of each of these substances, several samples are weighed in whose masses should be roughly equal to those recommended for the respective calorimeter and used for routine measurements.
- These samples are to be dealt with as described in Section 3.1.2, the smallest possible heating and cooling rates being, however, included.
- From the difference between the phase transition temperatures measured in the cooling mode and those expected due to the known supercooling, a table for the temperature correction in the cooling mode is compiled. $\Delta T_{corr}(\beta=0)=T_{tr}-T_{e/p}(\beta=0)$ is valid. (For an example, see Section 5.1.1).

The temperature calibration in the cooling mode has, thus, been performed. By analogy to the heating mode it is strictly valid only for the cooling rate zero. For finite cooling rates, the sample temperature is higher than the temperature displayed. It thus is necessary to construct a calibration table or curve

for all cooling rates applied, giving the differences between sample temperature and temperature displayed in dependence on the cooling rate. Generally, those corrections are insignificant for small cooling rates but can be important for higher ones (>5 K min^{-1}), and can, additionally, depend on the sample mass. The results of the calibration experiments can be used for compiling this table or curve. It is, however, also possible to use suitable pure substance showing a defined supercooling to obtain relative temperature differences as a function of the cooling rate. In this case, the same procedure is to be applied as during the calibration.

3.2. Heat flow rate calibration

3.2.1. Rationale for the procedure

Heat flow rate calibration in the cooling mode is performed by complete analogy to that in the heating mode. The substances recommended (Table 2) can also be used for calibration in the cooling mode. Due to the sample cooling which takes place as a result of thermal conduction, convection and radiation, the thermal lag generally is more pronounced in the cooling mode than in the heating mode. It therefore may happen that — according to the thermal diffusivity of the calibration substance used — the heat capacities measured in the cooling mode systematically differ from those measured in the heating mode, although the experiments are in both cases performed according to the same procedure. The higher the difference in thermal diffusivity, the greater the differences. It is recommended to separately examine this effect and to include it in the determination of the measurement uncertainty, if need be.

3.2.2. Performance of the calibration

Every measurement consists of three steps which can also be identified in the curve of measured values (see Fig. 1 for an example). To determine the starting line $\Phi_{iso,st}$, the measuring system is first kept isothermal; subsequently, the temperature interval of interest is traversed down to the final temperature at the desired cooling rate β (generally 10 K min^{-1}). Then, the end line, $\Phi_{iso,end}$, is determined in the isothermal state. The same temperature program is used for the measurement with crucibles empty Φ_0, and the calibration sample measurement, $\Phi_{S,cal}$.

If the isothermal starting and end lines of calibration sample measurement and measurement with crucibles empty are displaced in relation to each other, this will be corrected for by subtraction of two interpolated straight lines Φ_i. To obtain these, the heat flow rate value of the isothermal starting line at t_{st} and the heat flow rate value of the isothermal end line, extrapolated to t_{end}, are required. The transformation of the indicated heat flow rate $\Phi_d(t)$ into the shift-corrected heat flow rate $\Phi'_d(t)$ is performed

Table 2
Substances recommended for heat flow rate calibration in the cooling mode [4]

Substance	Temperature range (K)	Heat capacity[a] $C_p(T)$ in J g^{-1} K^{-1}	Uncertainty (%)	Remarks	Literature
Corundum (α-Al_2O_3)	70–300	$\sum_{i=0}^{7} a_i T^i$	0.4–0.1	NIST SRM 720[b] (synthetic sapphire)	[7]
	290–2250	$\sum_{i=0}^{7} b_i T^i$	0.1–0.2		
Copper (Cu)	20–97.5	$\sum_{i=0}^{6} c_i T^i$	0.1	OFHC quality[c]	[8]
	97.5–320	$\sum_{i=0}^{4} d_i T^i$	0.1		

[a] The polynomials given have also been adjusted at the limits of the respective temperature ranges with respect to the first derivative dC_p/dT.
[b] National Institute of Standards and Technology, USA, Standard Reference Material.
[c] Oxygen-free, high conductivity.

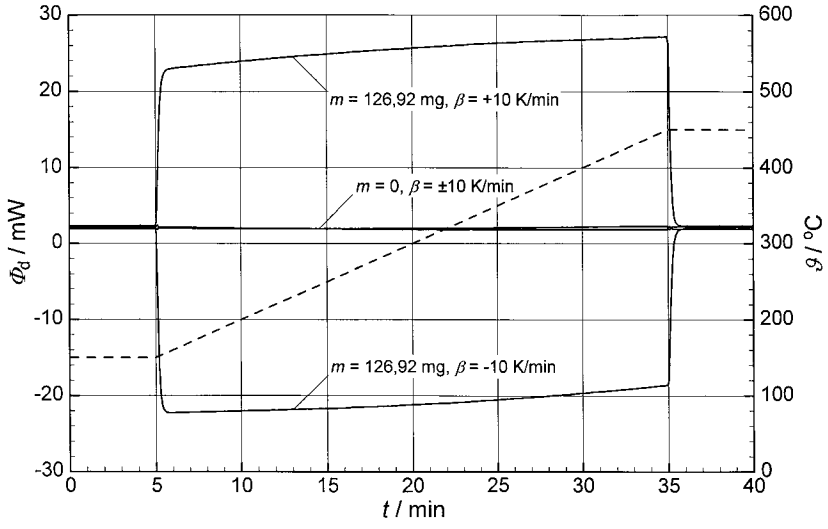

Fig. 1. Curves of measured values $\Phi_d(t)$ (continuous line) and $T(t)$ (dashed line) for the heat flow rate calibration of a power-compensated calorimeter in the heating and the cooling mode with crucibles empty and when a corundum sample with m=126.92 mg is used. The measurements with crucibles empty nearly coincide.

according to the formula

$$\Phi'_d(t) = \Phi_d(t) - \left(\Phi_{iso,st} + \frac{\Phi_{iso,end} - \Phi_{iso,st}}{t_{end} - t_{st}} (t - t_{st}) \right) \quad (1)$$

With the relationship $T=f(t)$, which is usually non-linear, the following is valid for the calibration factor for heat flow rate measurements $K_\Phi(T)$:

$$K_\Phi(T) = \frac{C_{S,cal}(T)\beta}{\Phi'_{S,cal}(T) - \Phi'_0(T)} \quad (2)$$

For the calibration, the following procedure is to be followed:

- The calibration substance is to be selected from Table 2 in dependence on the desired temperature range.
- Measurements are to be carried out with at least two calibration samples of different heat capacity C_p (mass); these are to be selected so that the heat capacity of the samples usually examined lies between the heat capacities of the calibration samples. Prior to each measurement of the calibration sample, a measurement with crucibles empty is to be carried out. Each calibration sample measurement and the associated measurement with crucibles empty should be carried out the same day.
- Measurement samples and calibration samples are to be weighed into crucibles which are as similar as possible or identical as regards shape, sealings, emissivities and masses.
- The time of the three steps of the temperature program must be selected so long that quasi-steady conditions are provided. This is the case after 3 to 10 times the time constant of the calorimeter in question to be taken from the curve of measured values (see Fig. 2 in [4]).
- Each individual measurement is to be repeated three times, and the same temperature program is to be used. The calibration sample measurements and the associated measurements with crucibles empty are to be carried out alternately.
- In the quasi-steady range, related pairs of values obtained from measurements with crucibles empty and from calibration sample measurements are to be evaluated according to Eq. (2), and mean values of $K_\Phi(T)$ are to be calculated for each sample. Differences in mass (heat capacity differences) of the crucibles used for the measurement with crucibles empty and for the measurement of the calibration sample are to be allowed for by computation.

3.3. Heat calibration

3.3.1. Rationale for the procedure

Heat calibration in the cooling mode is to be performed by complete analogy to that in the heating mode. The procedure is to be transferred to the cooling mode. For heat calibration, only substances that (with the unavoidable supercooling) do not show any significant or show a known temperature dependence of the phase transition enthalpy are suitable, and only such substances were included in Table 4. (The discussion there, and in the following, on the temperature dependence of the crystallisation enthalpy in liquid/solid phase transitions is valid by analogy for the temperature dependence of the transition enthalpy in solid/solid transitions).

3.3.2. Calibration procedure

The calibration is to be carried out as follows:

- The calibration substances are to be selected from Table 4 in dependence on the desired temperature range; their phase transition temperatures must be appropriately distributed over the temperature range of interest.
- Measurements are to be carried out with at least two calibration samples having different phase transition heats Q_{tr} (mass); the masses are to be selected so that the heat measured for the samples under investigation lies between the phase transition heat of the calibration samples. The calibration samples should be measured the same day.
- Samples under investigation and calibration samples are to be weighed into crucibles whose shapes, sealings and emissivities are as similar as possible or identical.
- According to the cooling rate selected (generally 5 K min^{-1}), the starting and the end temperatures for the calibration measurement are to be selected in such a way that the baseline between initial peak time t_i and final peak time t_f can be clearly interpolated. To achieve this, the scanning phase of the temperature program must be selected at least so long that quasi-steady conditions both before and after phase transition are provided.
- Each measurement is to be repeated three times, and the same temperature program is to be used. Each time the crucible with the calibration sample is to be removed from the measuring system, and placed back into it.
- For each individual measurement the calibration factor $K_Q(T)$ is to be calculated. For each sample (mass) the mean value of K_Q is computed:

$$K_Q(T_{trs}) = \frac{Q_{tr}}{Q_m} = \frac{Q_{tr}}{A}\frac{Q_{tr}}{\int_{t_i}^{t_f}[\Phi_m(t) - \Phi_{bl}(t)]\,dt} \stackrel{!}{=} \frac{\Delta_{trs}H(T_{trs})}{\int_{t_i}^{t_f}[\Phi_m(t) - \Phi_{bl}(t)]\,dt} \quad (3)$$

- $\Delta_{trs}H(T_{trs})$ is calculated according to Eq. (11) with the values for $\Delta_{trs}H$ and $\Delta_{trs}C_p(T)$ from Table 4.

4. Calibration substances

4.1. Requirements and rationale for the selection of the calibration substances for the cooling mode

The calibration substances should meet the following general requirements:

- The substance must be available with sufficient purity (no measurable influence of existing impurities on the phase transition temperature, phase transition heat or heat capacity).
- Reactions with crucible material, purge gas (ambient atmosphere) and photoreactions must not occur.
- The substance should be of long-term stability, non-hygroscopic and of low volatility.
- The substance should be physiologically safe.

For substances for temperature calibration, the following is additionally valid:

- The substances should realise, if possible, fixed points of the ITS-90. If additional substances are needed, their respective phase transition temperatures must be precisely measured and linked up with the ITS-90.
- The phase transition temperature must be clearly defined from the thermodynamics point of view.
- The grain sizes of the phases involved must not influence the phase transition temperature.
- Measurable supercooling must not occur (no influence of nucleation).
- The rate of transition must be high.

Additionally, the following is valid for calibration substances for heat and heat flow rate:

- The heat capacity or the phase transition heat should have been measured, if possible, using two different adiabatic calorimeters.

The following additional requirements are valid for heat calibration substances:

- The phase transition must be well-defined.
- The variation of the heat capacity during the phase transition should be small.
- The transition should be without supercooling (no influence of nucleation).
- A reliable best value must be available for the phase transition heat.

The following additional requirements are valid for heat flow rate calibration substances:

- No phase transition must occur in the temperature range traversed.
- Reliable fitting polynomials must be available for the heat capacity values.

The calibration substances recommended in the following tables do not always fulfil all the requirements listed above, on the contrary, due to the supercooling of crystallisation processes (see Section 5.2.1) and the need for a sufficiently great number of calibration substances, compromises must be made.

- A potential supercooling of a temperature calibration substance is considered negligible provided that it is smaller than 0.5 K.
- Indium shows small but reproducible supercooling, but nevertheless offers advantages for heat calibration and allows simultaneous calibration in the heating and cooling mode.
- Adamantane shows small but reproducible supercooling but in the low-temperature range it is one of the few substances recommended for temperature calibration.
- At the melting point, the vapour pressure of zinc is high. Zinc easily forms alloys with substances for the construction of calorimeters, but shows only little supercooling and, in the high-temperature range, therefore, is one of the few substances which can be recommended for simultaneous temperature and heat calibration in the heating and the cooling mode.

The supercoolings stated in Table 1 were obtained from measurements which had been performed by the authors with different substance charges in different crucibles as well as from a critical evaluation of the literature available.

4.2. Temperature calibration substances

Substances recommended for temperature calibration in the cooling mode are given in Table 1.

4.3. Substances for heat flow rate calibration

Substances recommended for heat flow rate calibration in the cooling mode and the coefficients of fitting polynomials for the heat capacity of the substances for heat flow rate calibration are given in Tables 2 and 3, respectively.

Table 3
Coefficients of fitting polynomials for the heat capacity of the substances for heat flow rate calibration [4]

i	a	b	c	d
0	3.63245×10^{-2}	-5.81126×10^{-1}	1.43745×10^{-2}	-1.63570×10^{-1}
1	-1.11472×10^{-3}	8.25981×10^{-3}	-1.21086×10^{-3}	7.07745×10^{-3}
2	-5.38683×10^{-6}	-1.76767×10^{-5}	-1.23305×10^{-5}	-3.78932×10^{-5}
3	5.96137×10^{-7}	2.17663×10^{-8}	4.20514×10^{-6}	9.60753×10^{-8}
4	-4.92923×10^{-9}	-1.60541×10^{-11}	-8.49738×10^{-8}	-9.36151×10^{-11}
5	1.83001×10^{-11}	7.01732×10^{-15}	6.71459×10^{-10}	
6	-3.36754×10^{-14}	-1.67621×10^{-18}	-1.94071×10^{-12}	
7	2.50251×10^{-17}	1.68486×10^{-22}		

Table 4
Substances recommended for heat calibration in the cooling mode

Substance	Phase transition temperature ϑ_{trs} (°C)	Phase transition enthalpy $\lvert\Delta_{trs}H\rvert$ (J g^{-1})	Temperature dependence[a] $d\Delta_{trs}H/dT = C''_p(T) - C'_p(T) = \Delta_{trs}C_p(T) = a + b(T - T_{trs})$		Literature
			a (J g^{-1} K^{-1})	b (J g^{-1} K^{-2})	
Cyclopentane	−150.77	69.60	+0.38	-5.8×10^{-3}	[4,9]
Cyclopentane	−135.09	4.91	−0.058	0	[4,9]
Cyclopentane	−93.43	8.63	+0.16	$+3.1\times10^{-3}$	[4,9]
Gallium	29.7646	79.88	+0.031	-4.6×10^{-4}	[4,10]
Indium	156.5985	28.62	−0.0026	-2.6×10^{-4}	[4,11,21]
Tin	231.928	60.40	−0.018	-3.1×10^{-4}	[4,12]
Zinc[b]	419.53	108.09	+0.012	-7.3×10^{-4}	[13,22]
Lithium sulfate	578.28	228.1	−0.15	-7.7×10^{-3}	[4,23]
Aluminium	660.323	398.1	−0.19	$+3.2\times10^{-4}$	[4,14]

[a] When Eq. (11) is used for the determination of the crystallisation enthalpy from the melting enthalpy, the signs of the quantities used are strictly to be taken into consideration: melting processes are endothermic and, therefore, melting enthalpies are positive; crystallisation processes are exothermic and, therefore, crystallisation enthalpies are negative. The signs of the given differences in heat capacity relate to the transition of the low-temperature phase to the high-temperature phase. Thus, for example, supercooling ($T - T_{fus} < 0$) leads to an increase in the crystallisation enthalpy when the heat capacity during the solid/liquid transition in the temperature interval decreases ($\Delta C_p < 0$). The crystallisation enthalpy being, however, negative, this means a reduction of the amount of the crystallisation enthalpy.

[b] Zn very easily reacts with aluminium which is usually used as crucible material (also when carefully oxidised). To avoid alloy formation with potential subsequent destruction of calorimeter components, it is therefore necessary to proceed very carefully and with great attention. It is advised to use only fresh samples, to examine the crucible bottom for cracks in the aluminium oxide layer, and to immediately cut short a series of experiments, as soon as during successive experiments an increase in the peak width or a decrease of the peak area is observed. The authors do not accept any responsibility for damages!

4.4. Heat calibration substances

Substances recommended for heat calibration in the cooling mode are given in Table 4.

5. Annex

5.1. Examples of calibration in the cooling mode

5.1.1. Example of temperature calibration

A power-compensated differential scanning calorimeter (Perkin-Elmer DSC-7) was — first in the heating mode — calibrated in the temperature range 0–300°C (270–570 K) using gallium, indium and tin, and the calibration curve shown in Fig. 2 was obtained (for $\beta = 0$).

Subsequently, the symmetry was examined as described in Section 3.1.2. M24, In, and $NaNO_3$ were selected as substances, two samples of each being weighed in. The masses were 0.5–2.1 mg; hermetically sealable aluminium crucibles were used. The heating and cooling rates were 2.5 and 10 K min^{-1}, respectively. According to Table 1, for the smectic/nematic transition of M24 and the solid/solid transition of $NaNO_3$, the peak extremum temperature T_p and for indium, the extrapolated peak-onset temperature T_e were evaluated. The results are compiled in Figs. 3–5. For this DSC and for the selected small masses this yields, in any case, a linear relation with the heating and cooling rate, respectively. For M24 and $NaNO_3$, the points of intersection of the regression lines coincide within an interval of 0.15 K. A difference of 1.8 K is recorded for indium, which corresponds to the usual supercooling of <2 K. It is, therefore, evident that the DSC is symmetrical in this temperature range as regards heating and cooling. A separate calibration in the cooling mode is not necessary; the calibration according to Fig. 2 is also valid in the cooling mode.

Note: differences in the slopes of the straight line for the cooling and the heating mode (see Fig. 5) stem from a certain time dependence of the phase transition, which is negligible for the verification of the symmetry.

5.1.2. Example of a heat flow rate calibration

A power-compensated differential scanning calorimeter (Perkin-Elmer DSC-2) was calibrated in the

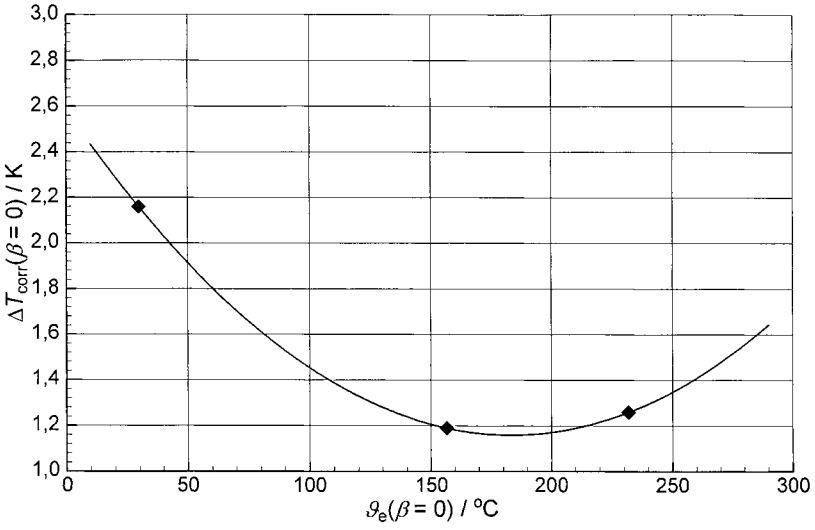

Fig. 2. Temperature calibration of a power-compensated differential scanning calorimeter in the heating mode.

temperature range between 150 and 450°C (423–723 K) using corundum (sample mass m=55.41 mg and m=126.92 mg). As crucibles, Al-pans with covers were used. With these samples the following temperature program was run as described in Section 3.2.2:

- initial isotherm: 5 min at 423 K;
- heating rate: 10 K min^{-1};
- final isotherm: 5 min at 723 K;
- initial isotherm: 5 min at 723 K;
- heating rate: −10 K min^{-1};
- final isotherm: 5 min at 423 K.

Fig. 1 exemplarily shows the curves of measured values for a calibration sample, Fig. 6 shows the heat flow rate calibration curves $K_\Phi(T)$ determined

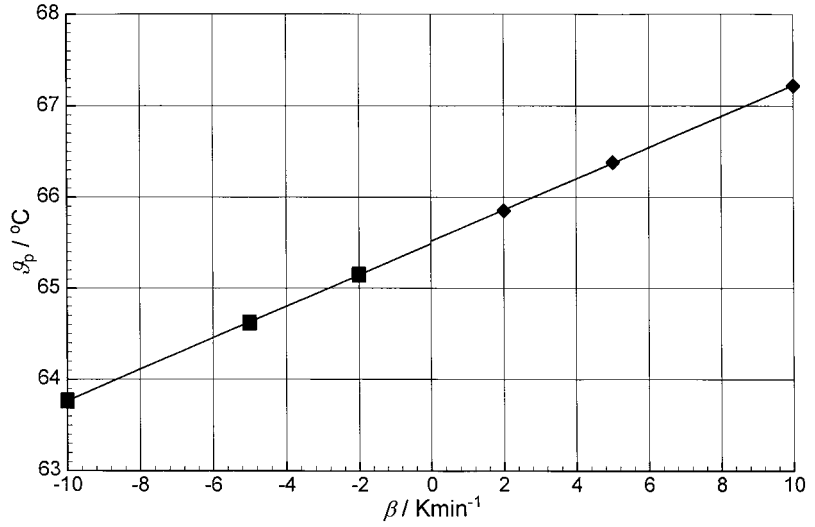

Fig. 3. Temperature calibration of a differential scanning calorimeter in the heating and the cooling mode using M24.

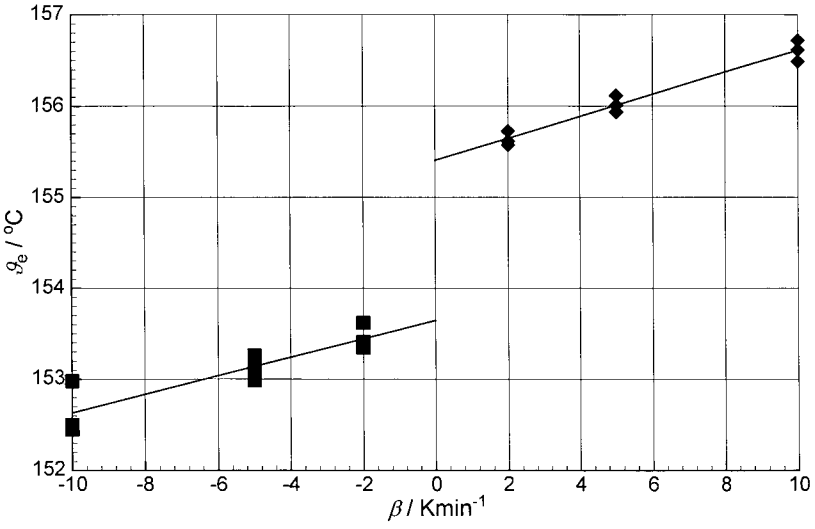

Fig. 4. Temperature calibration of a differential scanning calorimeter in the heating and the cooling mode using In.

according to Eq. (2) using a corundum sample with m=55.41 mg, and Fig. 7 for a corundum sample with m=126.92 mg.

5.1.3. Example of a heat calibration

A power-compensated differential scanning calorimeter (Perkin-Elmer DSC-2) was calibrated in the temperature range between 100 and 450°C (370–720 K) as described in Section 3.3.2. Before, a temperature and heat calibration in the heating mode according to the recommendations [4,16] as well as an examination of the symmetry of the temperature calibration in the cooling mode according to Section 3.1.2 were performed. The temperature calibration

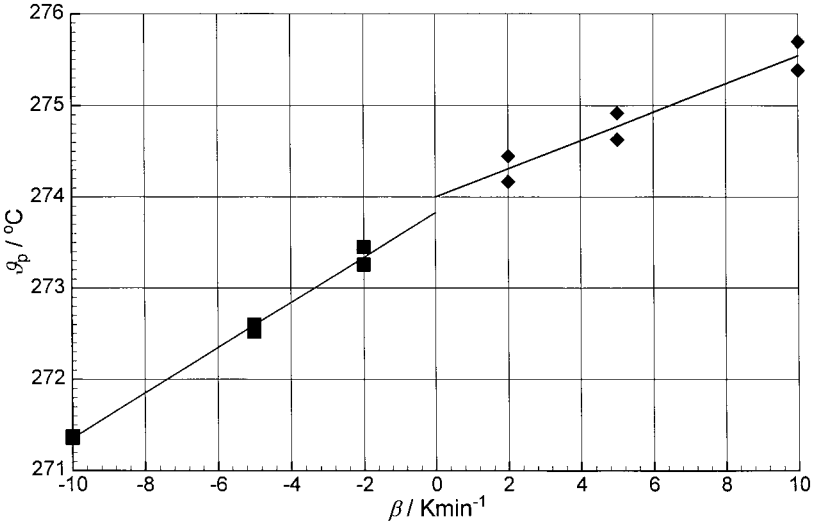

Fig. 5. Temperature calibration of a differential scanning calorimeter in the heating and the cooling mode using $NaNO_3$.

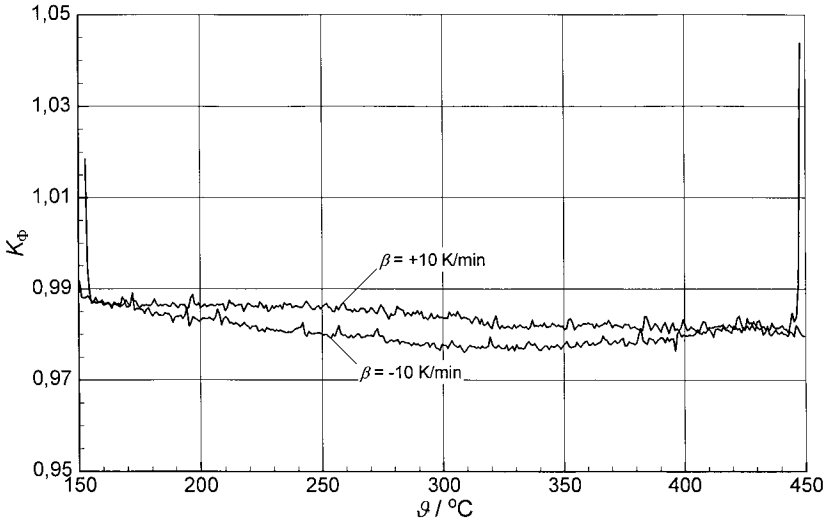

Fig. 6. Calibration curves $K_\Phi(T)$ averaged from three individual measurements each for a power-compensated calorimeter in the heating (above) and the cooling (below) mode using a corundum sample with m=55.41 mg.

showed an approximately constant dependence of the measured extrapolated peak-onset temperatures on the heating rate of $dT_e/d\beta$=6.2 s for metals. This value is needed for the determination of supercooling.

Indium and tin were selected for heat calibration in the cooling mode. Two samples of 1 and 5 mg were weighed into hermetically sealable aluminium crucibles. The heating rate was -5 K min^{-1}. The results of the calibration are compiled in Table 5.

Here supercooling during the crystallisation of indium is weak, and the contribution of the heat capacity difference correspondingly small. The deviation of the negative crystallisation enthalpy from the melting enthalpy, therefore, is within the uncertainty

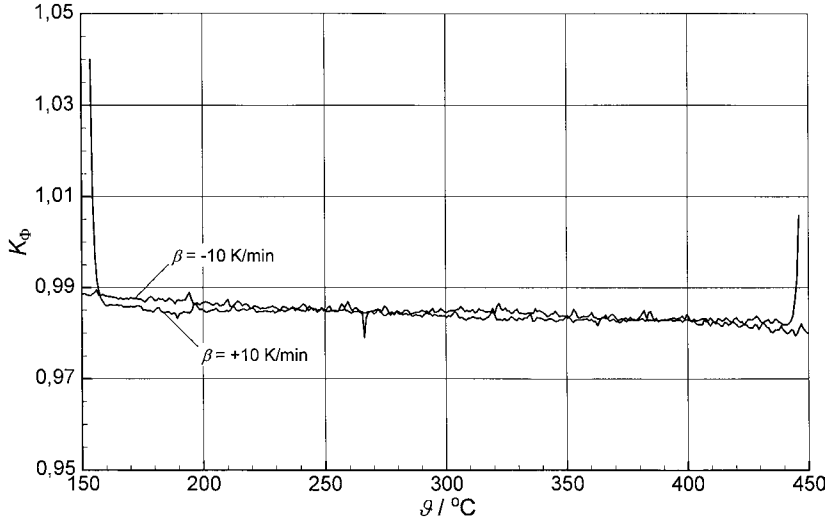

Fig. 7. Calibration curves $K_\Phi(T)$ averaged from three individual measurements each for a power-compensated calorimeter in the heating and the cooling mode using a corundum sample with m=126.92 mg. The calibration curves nearly coincide.

Table 5
Results of heat calibration in the cooling mode

Substance	m (mg)	ϑ_e (°C)	$\vartheta_e(\beta=0)$ (°C)	$T_{trs}-T_{fus}$ (K)	$\int \Delta C_p \, dT$ (J g^{-1})	$Q_{tr}(T_{trs})$ (J g^{-1})	Q_m (J g^{-1})	K_Q	$\overline{K}_Q$
In	0.996	154.62	155.14	−1.46	0.0035	−28.616	−28.434	1.006	1.003
		154.66	155.18	−1.42	0.0034	−28.617	−28.553	1.002	
		154.37	154.89	−1.71	0.0041	−28.616	−28.573	1.002	
	5.216	154.43	154.95	−1.65	0.0039	−28.616	−28.626	1.000	0.998
		154.58	155.09	−1.51	0.0036	−28.616	−28.653	0.999	
		154.46	154.98	−1.62	0.0039	−28.616	−28.769	0.995	
Zn	1.554	418.99	419.50	−0.03	0	−108.09	−106.703	1.013	1.007
		419.10	419.62	0.09	0	−108.09	−107.282	1.008	
		419.18	419.70	0.17	0	−108.09	−108.102	1.000	
	4.896	418.91	419.43	−0.10	0	−108.09	−107.922	1.002	1.004
		419.31	419.83	0.30	0	−108.09	−107.618	1.004	
		419.40	419.91	0.38	0	−108.09	−107.463	1.006	

of the melting enthalpy and has been determined here only for pedagogical reasons. In these experiments, the crystallisation temperatures for zinc scatter around the melting temperature. Supercooling is therefore set equal to 0, and the crystallisation enthalpy is equal to the negative melting enthalpy.

The comparison with the heat calibration factors determined in the heating mode (see Table 6) shows that within the scope of the uncertainty (here the standard deviation is given) the calorimeter is symmetrical with respect to heat determination in the heating and the cooling mode.

Note: During crystallisation, especially of substances tending to strong supercooling, very thin peaks may occur. This is why the greatest data acquisition rate possible should be selected in the cooling mode. To avoid unnecessarily great data quantities in the case of substances with strong supercooling, the high data acquisition rate should be activated only in the temperature range in which the crystallisation will likely occur.

Table 6
Comparison of heat calibration factors in the heating and the cooling mode

Substance	K_Q ($\beta>0$)	K_Q ($\beta<0$)
In	1.000±0.018	1.001±0.004
Zn	1.001±0.004	1.005±0.005

5.2. Theory, thermodynamics

5.2.1. Thermodynamic fundamentals as regards calibration in the cooling mode

For temperature and heat calibration phase transitions of pure substances are used. The knowledge necessary for understanding the recommended calibration procedures is compiled in the following.

The heat flow rate of a (calibration) sample generally is [15]

$$\frac{\delta Q}{dt} = \Phi = C_{p,\xi}(T)\beta + \left[\left(\frac{\partial H}{\partial p}\right)_{T,\xi} - V\right]\beta\frac{dp}{dT} + \left(\frac{\partial H}{\partial \xi}\right)_{T,p}\frac{d\xi}{dt} \quad (4)$$

As in scanning calorimetry the measurements are nearly exclusively performed isobarically (especially for calibration), the second addend in Eq. (4) is 0. The first addend provides the basis for the heat flow rate calibration according to Eq. (2). The third addend forms the basis for heat calibration, e.g. through phase transitions. For this, the solid/liquid transitions of pure substances (melting phase transitions) are well established and have proved their worth. The sample melts within an infinite small temperature interval, while $d\xi/dt$ increases from 0 to a finite value. As described in [16], this allows the measured extrapolated peak-onset temperature extrapolated to the heating rate zero, $T_e(\beta=0)$, to be compared with the

phase transition temperature T_{trs}, and, thus temperature calibration. The integral over the heat flow rate curve, corrected for the baseline, for complete extent of reaction (i.e. over the total melting peak) is related to the true melting enthalpy (calibration value) to determine the calibration factor for heat measurements, compare Eq. (3).

Although a multitude of phase transitions is available for calibration, melting phase transitions have proved to be suitable for scanning calorimeters. They count among the so-called *phase transitions of first order*. According to Ehrenfest, the order of a phase transition is classified according to the lowest derivative of Gibbs' energy $G(T,p,x)$, which shows a discontinuity (a leap) in this phase transition. Practically important cases are:

Gibbs' function and its derivatives	Phase transition of first order	Phase transition of second order
G	continuous	continuous
$\left(\frac{\partial G}{\partial T}\right)_p = -S; \left(\frac{\partial G}{\partial p}\right)_T = V; \left(\frac{\partial (G/T)}{\partial T}\right)_p = -\frac{H}{T^2}$	discontinuous	continuous
$\left(\frac{\partial^2 G}{\partial T^2}\right)_p = -\frac{C_p}{T}; \left(\frac{\partial^2 G}{\partial p_2}\right)_T = -\kappa V; \left(\frac{\partial^2 G}{\partial T \partial p}\right) = \alpha V$	discontinuous	discontinuous

This applies in analogy to phase transitions of higher than second order. Phase transitions of higher order are not, however, so clearly defined by thermodynamics as those of first order. In reality, some phase transitions behave like transitions of 'mixed' order.

From the continuity of G during phase transition, the known Clausius–Clapeyron equation (also called first Ehrenfest equation) results for first-order phase transitions:

$$\frac{\mathrm{d}p}{\mathrm{d}T} = \frac{\Delta_{trs}H}{T\Delta_{trs}V} \tag{5}$$

This equation gives the slope of the coexistence curve (intersection curve of the respective areas of state) of the phases involved. In Eq. (5), $\Delta_{trs}V$ is the change of the volume of the substance during the phase transition (e.g. change of the volume related to the amount of substance). $\Delta_{trs}H$ (in most cases also related to 1 mol) is the enthalpy change of the substance during the phase transition. According to the transition in question, it is called melting ($\Delta_{fus}H$), evaporation ($\Delta_{vap}H$), sublimation ($\Delta_{sub}H$) or phase transition enthalpy ($\Delta_{trs}H$).

As regards the temperature dependence of $\Delta_{trs}H$, literature very often says that it is calculated according to the Kirchhoff equation. This is, however, valid for the temperature dependence of reaction enthalpies and not for a lasting phase equilibrium. The difference of the corresponding so-called equilibrium heat capacities ΔC_{eq} is, on the contrary, calculated according to the equation of Planck, which is obtained by differentiation of the corresponding equation of Clausius–Clapeyron with respect to T. For the temperature dependence of the melting enthalpy at equilibrium pressure, the following relation thus is valid:

$$\frac{\mathrm{d}\Delta_{fus}H}{\mathrm{d}T} = \Delta_{fus}C_p + \frac{\Delta_{fus}H}{T} - \frac{\Delta_{fus}H}{\Delta_{fus}V}(\alpha_s V_s - \alpha_{liq}V_{liq}) \tag{6}$$

The dependence of the enthalpy of the two phases involved ("high-temperature phase," low-temperature phase) on temperature, pressure and extent of reaction is described by its total differential:

$$\mathrm{d}H'' = \left(\frac{\partial H''}{\partial T}\right)_{p,\xi}\mathrm{d}T + \left(\frac{\partial H''}{\partial p}\right)_{T,\xi}\mathrm{d}p + \left(\frac{\partial H''}{\partial \xi}\right)_{T,p}\mathrm{d}\xi \tag{7}$$

$$\mathrm{d}H' = \left(\frac{\partial H'}{\partial T}\right)_{p,\xi}\mathrm{d}T + \left(\frac{\partial H'}{\partial p}\right)_{T,\xi}\mathrm{d}p + \left(\frac{\partial H'}{\partial \xi}\right)_{T,p}\mathrm{d}\xi \tag{8}$$

When a supercooled melt begins to crystallise, the two phases are not in equilibrium with each other; on the contrary, the dependence on temperature, pressure and extent of reaction must here be taken into account. Since it can be assumed under the conditions prevailing in scanning calorimetry that the pressure is (nearly) constant, the second term of Eqs. (7) and (8) can be neglected ($dp=0$). In a binary system, $dH'=-dH''$ and $d\xi'=-d\xi''$, so the third term of Eqs. (7) and (8) cancels as well.

By definition, $(\partial H/\partial T)_{p,\xi} \equiv C_{p,\xi}$ and $H''-H' \equiv \Delta_{trs}H$.

If the heat capacities of the two phases depend themselves on temperature, Eq. (9) then follows by subtraction of Eq. (8) from Eq. (7):

$$\frac{d\Delta_{trs}H}{dT} = C_p''(T) - C_p'(T) = \Delta_{trs}C_p(T) \tag{9}$$

After integration, this equation furnishes the temperature dependence of the phase transition enthalpy searched. If, for example, the heat capacities of the two phases involved are linear functions of temperature ($C_p'(T) = a' + b'T$ and $C_p''(T) = a'' + b''T$, respectively), the difference in heat capacity is also a linear function of supercooling ($\Delta_{trs}C_p(T)=a+b(T-T_{fus})$, cf. Section 5.4). As a result, the integration yields the crystallisation enthalpy at the crystallisation temperature $\Delta_{trs}H(T_{trs})$ from the crystallisation enthalpy at the melting temperature $\Delta_{trs}H(T_{fus})$ and the coefficients of the $\Delta_{trs}C_p$ function:

$$\Delta_{trs}H(T_{trs}) = \Delta_{trs}H(T_{fus}) + (a - bT_{fus})(T_{trs} - T_{fus}) + \tfrac{1}{2}b(T_{trs}^2 - T_{fus}^2) \tag{10}$$

With $\Delta_{trs}H(T_{fus})=-\Delta_{fus}H(T_{fus})$, the following relation is obtained:

$$\Delta_{trs}H(T_{trs}) = -\Delta_{fus}H(T_{fus}) + (a - bT_{fus})(T_{trs} - T_{fus}) + \tfrac{1}{2}b(T_{trs}^2 - T_{fus}^2) \tag{11}$$

In second-order phase transitions, the continuity of the first derivatives of G yields the continuity of the functions S, V and H at the phase transition; thus there is neither a phase transition entropy ($\Delta_{trs}S=0$) nor a phase transition enthalpy ($\Delta_{trs}H=0$) nor a change in volume ($\Delta_{trs}V=0$). The second equations of Ehrenfest thus are:

$$\frac{dp}{dT} = \frac{\Delta_{trs}C_p}{VT\Delta_{trs}\alpha} \quad \text{and} \quad \frac{dp}{dT} = \frac{\Delta_{trs}\alpha}{\Delta_{trs}\kappa} \tag{12}$$

whereas, in this case, Eq. (5) furnishes the uncertain expression 0/0.

These phase transitions may extend over a greater temperature range, while the enthalpy changes continuously. Often, the slope of its derivative (C_p) first increases continuously, and then decreases again (a transition showing this kind of $C_p(T)$ function is called an Λ-transition). Thus there is an anomaly of the $C_p(T)$ function which naturally is identical in the heating and the cooling mode (no supercooling). In these cases, the phase transition temperature is the temperature at which the slope of the heat capacity/temperature function changes its sign. For Λ-transitions this is the peak extremum temperature.

Due to the structural change which is always involved, real phase transitions obviously show always a hysteresis. The greater the structural change and $\Delta_{trs}V$ and $\Delta_{trs}\alpha$, respectively, the more marked the hysteresis. In this nucleation barrier thus produced — above all in phase transitions of first order — volume, surface and elastic components are involved. The nucleation procedure is followed by the macroscopic development of the nuclei into the new phase. It is one of the special features of the behaviour of solids that phase transitions can hardly ever be superheated, but very often supercooled; the more considerable the structural change, the more marked, generally, this phenomenon.

As to the microscopic nature of the occurring structural change, for solid/solid transitions, a distinction is made between positional, orientation and electron or nuclear spin transitions. In the same order, the impediments to the adjustment of a new state of phase decrease. That means that especially great (and above all in most cases non-reproducible) supercoolings occur during crystallisation of the melt, i.e. however, when those processes which in the case of calibration with positive heating rates are often successfully used are reversed. If, however, the melting process of a solid is interrupted in time (e.g. by changing from the heating to the cooling mode in the calorimeter), so that a remainder of unmolten solid phase is left, this can again increase with the subsequent decrease of the furnace temperature, thus serving as nucleus.

It is thus reasonable to look for substances with phase transitions higher than of first order and with as small a structural change as possible for the calibration in the cooling mode. This is, however, practical for

temperature calibration, but due to the small change in heat capacity involved it frequently leads to so small signals that a small signal-to-noise ratio results.

According to these principles, the authors took into account a number of substances most of which they rejected after thorough examinations. Some examples are: plastic crystals, substances with orientation transitions (SiO_2, $NaNO_2$, NH_4Cl, phenanthrene), with crystallisation to highly disordered solid phases (among others, long-chain *n*-alkanes), and with mesophase transitions (in particular phase transitions of thermotropic liquid crystals, here above all the liquid/smectic transition).

From the above-mentioned characteristics of all these transitions which are not of first order, it results that, in these cases, not the extrapolated peak-onset temperature T_e (the determination of which is very uncertain or even impossible) but the peak extremum temperature T_p is to be used as the characteristic temperature for temperature calibration.

5.2.2. *Mass and heating rate dependence of the peak extremum temperature*

Heat transport takes time. In a differential scanning calorimeter this results in temperature gradients and a lag of the sample temperature after the program temperature. In the case of an endothermic phase transition, the heat consumption increases strongly and the sample temperature drops even more behind the program temperature. In the extreme case of a first-order phase transition of a pure substance, the sample temperature remains approximately constant until the phase transition of the sample is completed and then — following an exponential law — it relaxes to the temperature lagging only due to the heat capacity of the sample. During melting this leads to an endothermic DSC signal as depicted in an idealised form in Fig. 8. In the exothermic crystallisation of a substance, the sign of the peak is reversed in the first approximation and the following argumentation applies by analogy.

With the beginning of the transition (at T_e), the sample temperature remains constant, whereas the inert reference substance continues to be linearly heated. Thus, the difference temperature between sample and reference substance also increases linearly and reaches the maximum value at the end of the phase transition, and then drops again exponentially to 0. While the 'extrapolated peak onset' of the transition characterises the very beginning of melting at the crucible bottom, and therefore does not depend on sample size and transition heat but only on the heating rate β and the heat transfer to the sample, this is not valid for the peak maximum (T_p).

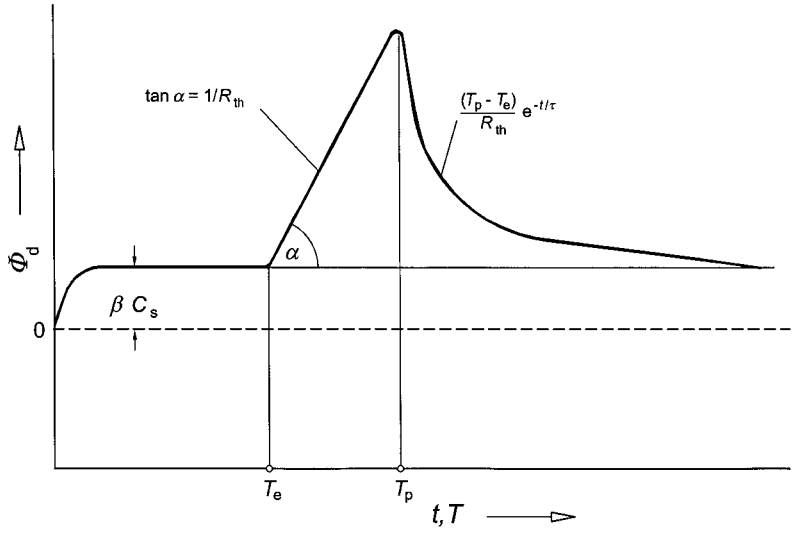

Fig. 8. Schematic description of a melting peak. *t*: time; *T*: temperature; β: heating rate; R_{th}: thermal resistance; C_S: heat capacity of the sample; T_e: extrapolated peak-onset temperature; T_p: peak maximum temperature; Φ_d: displayed heat flow rate; τ: signal time constant, α: angle.

For the difference $T_p - T_e$ (see Fig. 8), peak integration and elementary conversions taking into account that the slope of the left flank is proportional to the reciprocal effective thermal resistance R_{th} ($d\Phi/dT = \beta(t_p - t_e)/[R_{th} \times (T_p - T_e)] = 1/R_{th}$) yield the following quantitative relation [17,18]:

$$T_p - T_e = -\tau\beta + \sqrt{\tau^2\beta^2 + 2mq_{trs}R_{th}\beta} \quad (13)$$

For the peak temperature, the following equation is obtained:

$$T_p = T_e(\beta) - \tau\beta + \sqrt{\tau^2\beta^2 + 2mq_{trs}R_{th}\beta} \quad (14)$$

Since the extrapolated peak-onset temperature typically depends linearly on β [16,17], Eq. (14) can be written as follows:

$$T_p = T_e(\beta = 0) + (c_1 - \tau)\beta + \sqrt{\tau^2\beta^2 + 2mq_{trs}R_{th}\beta} \quad (15)$$

According to the size of the constants c_1, τ, R_{th} and q_{trs} which depend on the apparatus and the sample, a more or less non-linear dependence on β or $\sqrt{mq_{trs}R_{th}\beta}$ results. At a small mass m, a small specific transition heat q_{trs} and a small effective thermal resistance R_{th}, the second term of Eq. (15) will predominate; for extrapolation to the heating rate $\beta = 0$, T_p is to be plotted as a function of β. For poorly heat-conducting samples with great transition heat, the third term of Eq. (15) will predominate, and T_p is to be plotted as a function of $\sqrt{mq_{trs}R_{th}\beta}$.

Both approximations can gain importance for the substances suggested and the procedure recommended here.

5.3. Temperature calibration by means of partial melting

Supercooling during crystallisation of the pure substances usually used for the calibration in the heating mode will not occur if a sufficient number of nuclei is available for homogeneous crystal growth. In the trivial case, these nuclei consist of the same material as the crystallising substance, i.e. the crystallisation of the liquid phase is initiated as long as some of the solid initial phase is still available [3,19].

In the scanning calorimeter this situation can be created by switching the temperature program from the heating to the cooling mode as long as the sample has not completely melted, i.e. the peak end has not yet been reached taking the inertia of the system into account. As crystallisation temperature, here the intersection of the extrapolated final base line of the crystallisation peak with the tangent at the falling peak flank is defined (see Fig. 9).

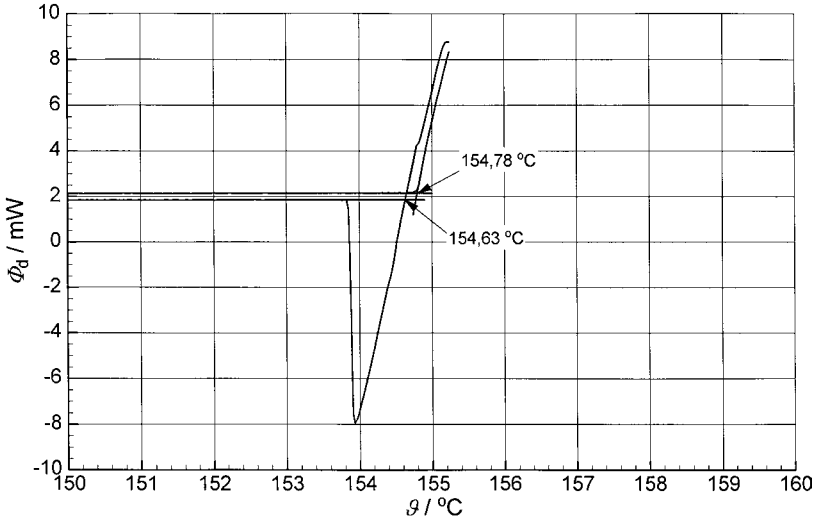

Fig. 9. Determination of extrapolated peak-onset temperatures for partial melting and recrystallisation for indium.

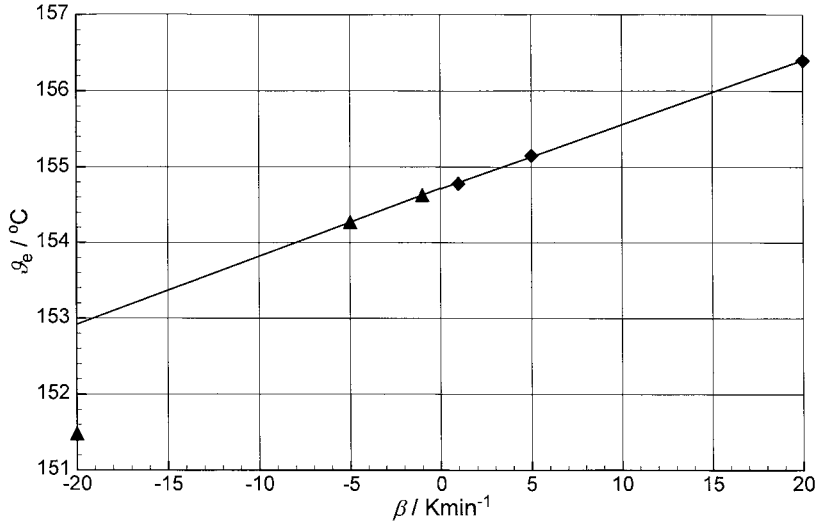

Fig. 10. Extrapolated peak-onset temperature as a function of the heating rate for indium for a power-compensated calorimeter. The calorimeter works symmetrically (the value measured at $\beta = -20$ K min^{-1} was not taken into account in the construction of the regression line).

It is of advantage that temperature calibration can be carried out in the heating and the cooling mode with one experiment.

A prerequisite for the performance of this procedure, namely the determination of the extrapolated peak-onset temperature as a function of the heating rate and extrapolation to the heating rate zero, is a calorimeter which reacts fast enough to the reversal of the heating rate so that the cooling rate specified is safely reached at the extrapolated peak-onset time.

Furthermore, this procedure requires a greater number of preliminary tests to determine the optimum time for switching from heating to cooling for the auto-

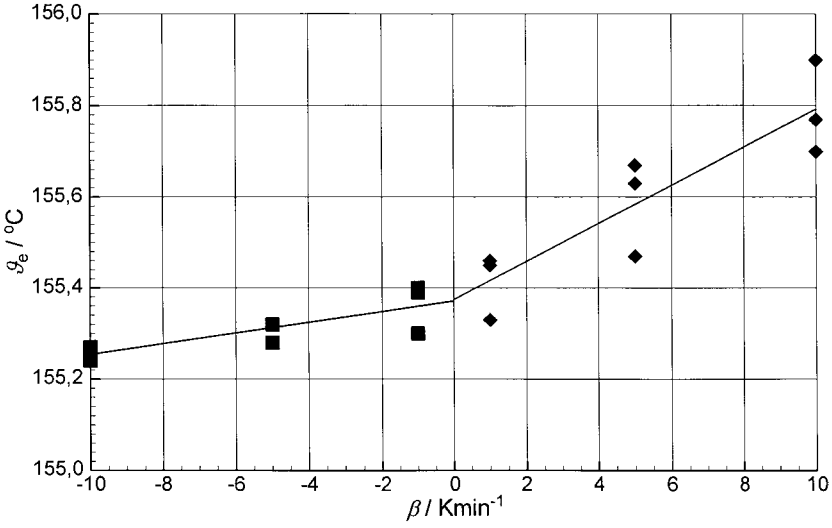

Fig. 11. Extrapolated peak-onset temperature as a function of the heating rate for indium for a heat flow calorimeter. The asymmetry is the result of the thermal inertia of the furnace which cannot realise the specified cooling rates fast enough.

Table 7
Specific heat capacities of the heat calibration substances

Substance	Phase	T_1 (K)	T_2 (K)	a' and a'', respectively (J g^{-1} K^{-1})	b' and b'', respectively (J g^{-1} K^{-2})	Literature
Cylopentane	I (solid)	86	120	0.322	5.33×10^{-3}	[9]
	II (solid)	124	135	1.434	-6.63×10^{-4}	
	III (solid)	141	173	1.385	-7.35×10^{-4}	
	Liquid	184	212	0.990	2.35×10^{-3}	
Gallium	Solid	273	303	0.306	2.29×10^{-4}	[10]
	Liquid	288	303	0.467	-1.97×10^{-4}	
Indium	Solid	328	429	0.176	1.90×10^{-4}	[11,21]
	Liquid	431	547	0.288	-7.51×10^{-5}	
Tin	Solid	440	500	0.139	2.52×10^{-4}	[12]
	Liquid	520	600	0.275	-5.43×10^{-5}	
Zinc	Solid	673	692	−0.027	7.31×10^{-4}	[22]
	Liquid	693	773	0.492	0	
Lithium sulfate	I (solid)	804	846	−3.799	7.22×10^{-3}	[23]
	II (solid)	866	913	2.645	-5.12×10^{-4}	
Aluminium	Solid	800	932	0.452	8.62×10^{-4}	[14]
	Liquid	933	1100	−0.037	1.18×10^{-3}	

matic performance of the measurement or the manual intervention of the user.

For these reasons, this procedure cannot be recommended at present. However, it can be assumed that decreasing thermal inertia of modern calorimeter furnaces and increasingly efficient control programs will lead to this procedure in future gaining in importance and being more widely applicable.

The figures show measurements for checking the symmetry according to Section 3.1.2 for a power-compensated (Fig. 10) and a heat flow calorimeter (Fig. 11).

5.4. Specific heat capacities of the heat calibration substances

The specific heat capacities of the heat calibration substances were taken from literature and approximated in the temperature range given by T_1 and T_2, by means of equations of the type $C'_p = a' + b' \times T$ and $C''_p = a'' + b'' \times T$.

As mostly no values are known for the heat capacity of the high-temperature phase in the supercooled state, the appropriate values were determined by extrapolation. The coefficients for $d\Delta_{trs}H/dT$ given in Table 4 result from the difference in the heat capacities of high-temperature and low-temperature phase according to $a=(a''-a')+(b''-b')T_{trs}$ and $b=b''-b'$, respectively, according to Table 7.

References

[1] S.-S. Chang, E.F. Westrum Jr., Heat capacities and thermodynamic properties of globular molecules. I. Adamantane and hexamethylentetramine, J. Phys. Chem. 64 (1960) 1547–1551.
[2] E.F. Westrum Jr., The thermophysical properties of three globular molecules, J. Phys. Chem. Solids 18 (1961) 83–85.
[3] P. Skoglund, Å. Fransson, Accurate temperature calibration of differential scanning calorimeters, Thermochim. Acta 276 (1996) 27–39.
[4] S.M. Sarge, E. Gmelin, G.W.H. Höhne, H.K. Cammenga, W. Hemminger, W. Eysel, The caloric calibration of scanning calorimeters, Thermochim. Acta 247 (1994) 129–168.
[5] G.J. Janz, F.J. Kelly, J.L. Pérano, Melting and pre-melting phenomena in alkali metal nitrates, J. Chem. Eng. Data 9 (1964) 133–136.
[6] Internationale Praktische Temperaturskala von 1968. Verbesserte Ausgabe von 1975, PTB-Mitt. 87 (1977) 497–510.
[7] D.A. Ditmars, S. Ishihara, S.S. Chang, G. Bernstein, E.D. West, Enthalpy and heat capacity standard reference material. Synthetic sapphire (α-Al_2O_3) from 10 to 2250 K, J. Res. Nat. Bur. Stand. 87 (1982) 159–163.

[8] D.L. Martin, 'Tray' type calorimeter for the 15–300 K temperature range: copper as a specific heat standard in this range, Rev. Sci. Instrum. 58 (1987) 639–646.
[9] J.G. Aston, H.L. Fink, S.C. Schumann, The heat capacity and entropy, heats of transition, fusion and vaporization and the vapor pressures of cyclopentane. Evidence for a non-planar structure, J. Am. Chem. Soc. 65 (1943) 341–346.
[10] E.B. Amitin, Yu.F. Mimenkov, O.A. Nabutovskaya, I.E. Paukov, S.I. Sokolova, Thermodynamic properties of gallium from 5 to 320 K, J. Chem. Thermodyn. 16 (1984) 431–436.
[11] F. Grønvold, Heat capacity of indium from 300 to 1000 K. Enthalpy of fusion, J. Thermal Anal. 13 (1978) 419–428.
[12] F. Grønvold, Heat capacity and thermodynamic properties of metallic tin in the range 300 to 1.000 K. Fusion characteristics, Rev. Chim. Min. 11 (1974) 568–584.
[13] S. Stølen, F. Grønvold, Review. Critical assessment of the enthalpy of fusion of metals used as enthalpy standards at moderate to high temperatures, Thermochim. Acta 327 (1999) 1–32.
[14] R.A. McDonald, Enthalpy, heat capacity, and heat of fusion of aluminium from 366 to 1647 K, J. Chem. Eng. Data 12 (1967) 115–118.
[15] I. Prigogine, R. Defay, Chemical Thermodynamics, Longmans, Green & Co., London, 1954, 24–25.
[16] G.W.H. Höhne, H.K. Cammenga, W. Eysel, E. Gmelin, W. Hemminger, The temperature calibration of scanning calorimeters, Thermochim. Acta 160 (1990) 1–12.
[17] K.-H. Illers, Die Ermittlung des Schmelzpunktes von kristallinen Polymeren mittels Wärmeflußkalorimetrie (DSC), Eur. Polym. J. 10 (1974) 911–916.
[18] W.F. Hemminger, S.M. Sarge, The baseline construction and its influence on the measurement of heat with differential scanning calorimeters, J. Thermal Anal. 37 (1991) 1455–1477.
[19] J.H. Flynn, Instrumental limitations upon the measurement of temperature and rate of energy production by differential scanning calorimetry, in: Thermal Analysis, Vol. 1, Proceedings of the 3rd ICTA, 23–28 August 1971, Davos, Switzerland, Birkhäuser, Basel, 1971, pp. 127–138.
[20] G. Hakvoort, C.M. Hol, DSC calibration during cooling, J. Thermal Anal. Cal. 56 (1999) 717–722.
[21] F. Grønvold, Enthalpy of fusion and temperature of fusion of indium and redetermination of the enthalpy of fusion of tin, J. Chem. Thermodyn. 25 (1993) 1133–1144.
[22] D.A. Ditmars, Calibration standards for differential scanning calorimetry. I. Zinc: absolute calorimetric measurement of T_{fus} and $\Delta_{fus}H_m$, J. Chem. Thermodyn. 22 (1990) 639–651.
[23] J. Nölting, V. Freystein, personal communication, 1993.